Single top quark production at D0

S. Jabeen([1])

For the D0 collaboration.

([1]) *Boston University*

Summary. — We present first evidence for the production of single top quarks at the Fermilab Tevatron $p\bar{p}$ collider. Using a 0.9 fb^{-1} dataset, we apply a multivariate analysis to separate signal from background and measure cross section for single top quark production. We use the cross section measurement to directly determine the CKM matrix element that describes the Wtb coupling. We also present results of W' and charged Higgs searches with the same final states as standard model single top quark production.

PACS 14.65.Ha; 12.15.Ji; 13.85.Qk; 14.70.Pw;12.60.Fr – list

1. – Introduction

Top quarks were first observed in strong $t\bar{t}$ pair production at the Tevatron collider in 1995 [1]. In the standard model (SM), $\sigma(p\bar{p} \to t\bar{t}+X) = 6.8^{+0.6}_{-0.5}$ pb at $\sqrt{s} = 1.96$ TeV for a top quark mass of 175 GeV. Top quarks are also expected to be produced singly via the electroweak processes illustrated in Fig. 1. For brevity, we use the notation "tb" to represent the sum of $t\bar{b}$ and $\bar{t}b$, and "tqb" for the sum of $tq\bar{b}$ and $\bar{t}\bar{q}b$. The next-to-leading order prediction for the s-channel single top quark cross section is $\sigma(p\bar{p} \to tb+X) = 0.88 \pm 0.11$ pb, and for the t-channel process, the prediction is $\sigma(p\bar{p} \to tqb+X) = 1.98 \pm 0.25$ pb.
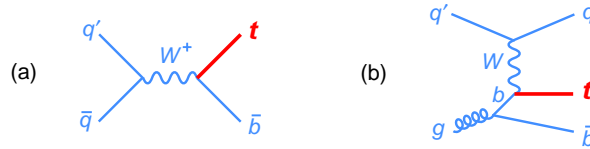

Fig. 1. – Representative Feynman diagrams for (a) s-channel single top quark production and (b) t-channel production.

Single top quark events can be used to study the Wtb coupling and to measure the magnitude of the CKM matrix element $|V_{tb}|$ without assuming only three generations of quarks. A value inconsistent with the SM expectation $|V_{tb}| \simeq 1$ would be a signature for new physics such as a fourth quark family. Single top quark production can also be used to measure the top quark partial decay width and hence the top quark lifetime.

2. – First Evidence for Single Top Quark and First Direct Measurement of Vtb

We describe a search for single top quark production using 0.9 fb^{-1} of data [2] collected from 2002 to 2005 using the D0 detector with triggers that required a jet and an electron or muon. The search focuses on the final state consisting of one high transverse momentum (p_T) isolated lepton and missing transverse energy ($\not{E}_T$), together with a b-quark jet from the decay of the top quark ($t{\rightarrow}Wb{\rightarrow}\ell\nu b$). There is an additional b quark in s-channel production, and an additional light quark and b quark in t-channel production. The second b quark in the t-channel is rarely reconstructed since it is produced in the forward direction with low transverse momentum. The main backgrounds are: W bosons produced in association with jets; top quark pairs in the lepton+jets and dilepton final states, when a jet or a lepton is not reconstructed; and multijet production, where a jet is misreconstructed as an electron or a heavy-flavor quark decays to a muon that is misidentified as isolated from the jet.

We model the signal using the SINGLETOP next-to-leading order Monte Carlo (MC) event generator. The event kinematics for both s-channel and t-channel reproduce distributions found in next-to-leading order calculations [3]. The decays of the top quark and resulting W boson, with finite widths, are modeled in the SINGLETOP generator to preserve particle spin information. PYTHIA is used to model the hadronization of the generated partons. For the tb (tqb) search, we assume SM tqb (tb) as part of the background model, and for the $tb+tqb$ search, we assume the SM ratio between the tb and tqb cross sections.

We simulate the $t\bar{t}$ and W+jets backgrounds using the ALPGEN leading-order MC event generator with parton-jet matching algorithm and PYTHIA to model the hadronization. The $t\bar{t}$ background is normalized to the integrated luminosity times the predicted $t\bar{t}$ cross section. The multijet background is modeled using data that contain nonisolated leptons but which otherwise resemble the lepton+jets dataset. The W+jets background, combined with the multijet background, is normalized to the lepton+jets dataset separately for each analysis channel (defined by lepton flavor and jet multiplicity) before b-jet tagging (described later). In the W+jets background simulation, we scale the $Wb\bar{b}$ and $Wc\bar{c}$ components by a factor of 1.50 ± 0.45 to better represent higher-order effects. This factor is determined by fitting an admixture of light- and heavy-flavor W+jets MC events to data that have no b tags but which otherwise pass all selection cuts. The uncertainty assigned to this factor covers the expected dependence on event kinematics and the assumption that the scale factor is the same for $Wb\bar{b}$ and $Wc\bar{c}$.

We select 1,398 b-tagged lepton+jets data events, which we expect to contain 62 ± 13 single top quark events. To increase the search sensitivity, we divide these events into twelve independent analysis channels based on the lepton flavor (e or μ), jet multiplicity (2, 3, or 4), and number of identified b jets (1 or 2). We do this because the signal acceptance and signal-to-background ratio differ significantly from channel to channel. The acceptances for single top quark signal as percentages of the total production cross sections are $(3.2 \pm 0.4)\%$ for tb and $(2.1 \pm 0.3)\%$ for tqb.

The dominant contributions to the uncertainties on the backgrounds come from: normalization of the $t\bar{t}$ background (18%), which includes a term to account for the top quark mass uncertainty; normalization of the W+jets and multijet backgrounds to data (17–27%), which includes the uncertainty on the heavy-flavor fraction of the model; and the b-tagging probabilities (12–17% for double-tagged events). The uncertainty on the integrated luminosity is 6%; all other sources contribute at the few percent level. The

uncertainties from the jet energy scale corrections and the b-tagging probabilities affect both the shape and normalization of the simulated distributions.

To separate the signal from background and thus enhance the probability to observe single top quarks we use three multivariate techniques: decision trees with adaptive boosting, matrix elements, and Bayesian neural networks. We identify 49 variables from an analysis of the signal and background Feynman diagrams and a study of single top quark production at next-to-leading order. The variables may be classified into three categories: individual object kinematics, global event kinematics, and variables based on angular correlations.

We use a boosted decision tree in each of the twelve analysis channels for three searches: $tb+tqb$, tqb, and tb. These 36 decision trees are trained to separate one of the signals from the sum of the $t\bar{t}$ and W+jets backgrounds. The second technique calculates the probability for each event to be signal or background based on the leading-order matrix element description of each process for two-jet and three-jet events. It takes as input the four-momenta of the reconstructed objects and incorporates the b-tagging information for each event. The third alternative method uses Bayesian neural networks to separate $tb+tqb$ signal from background. We train the networks on signal and background events in their measured proportions separately for each analysis channel, using 24 input variables (a subset of the 49 used in the boosted decision tree analysis). Large numbers of networks are averaged, resulting in better separation than can be achieved with a single network. Figure 2 shows the sum of the 12 $tb+tqb$ outputs for three analyses
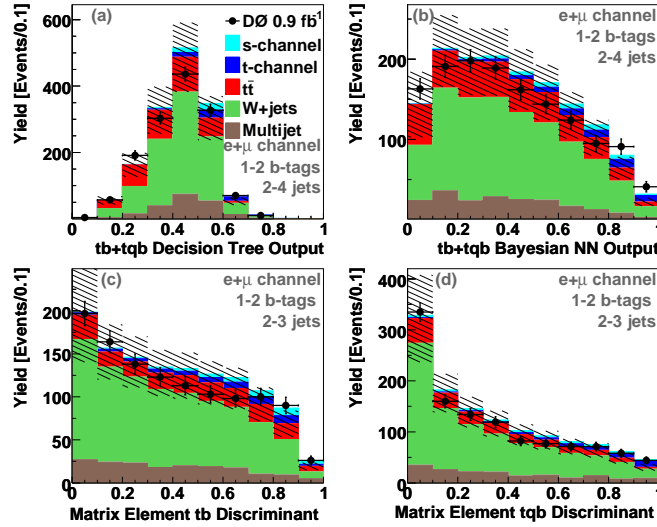

Fig. 2. – The discriminant outputs of the three multivariate discriminants: (a) DT, (b) BNN, (c) ME s-channel, and (d) ME t-channel discriminants. The signal component is normalized to the cross section measured from data in each case. The hatched bands show the 1 σ uncertainty on the background.

We apply a Bayesian approach to measure the single top quark production cross section. We form a binned likelihood as a product over all bins and channels (lepton flavor, jet multiplicity, and tag multiplicity) of all the discriminants for all channels separately.

We assume a Poisson distribution for the observed counts and flat nonnegative prior probabilities for the signal cross sections. Systematic uncertainties and their correlations are taken into account by integrating over the signal acceptances, background yields, and integrated luminosity with Gaussian priors for each systematic uncertainty. The final posterior probability density is computed as a function of the production cross section. For decision trees analysis we use the measured posterior density distributions to make the following measurements: $\sigma(p\bar{p} \rightarrow tb + X, \ tqb + X) = 4.9 \pm 1.4$ pb, $\sigma(p\bar{p} \rightarrow tqb + X) = 4.2^{+1.8}_{-1.4}$ pb, and $\sigma(p\bar{p} \rightarrow tb + X) = 1.0 \pm 0.9$ pb. These results are consistent with the SM expectations. The uncertainties include statistical and systematic components combined. The data statistics contribute 1.2 pb to the total 1.4 pb uncertainty on the $tb+tqb$ cross section. For the matrix element analysis we measure $\sigma(p\bar{p} \rightarrow tb + X, \ tqb + X) = 4.8^{+1.6}_{-1.4}$ pb and for the Bayesian neural network analysis we measure $\sigma(p\bar{p} \rightarrow tb + X, \ tqb + X) = 4.4^{+1.6}_{-1.4}$ pb.

We combine these three measurements and measure the cross section to be

$$\sigma\left(p\bar{p} \rightarrow tb + X, \ tqb + X\right) = 4.7 \pm 1.3 \text{ pb}.$$

This corresponds to an excess of 3.6 Gaussian-equivalent standard deviation significance and constitutes the first evidence of a single top quark signal. Ensemble tests have shown this result to be compatible with the standard model cross section with 10% probability.

We use the decision tree measurement of the $tb+tqb$ cross section to derive a first direct measurement of the strength of the $V-A$ coupling $|V_{tb}f_1^L|$ in the Wtb vertex, where f_1^L is an arbitrary left-handed form factor.
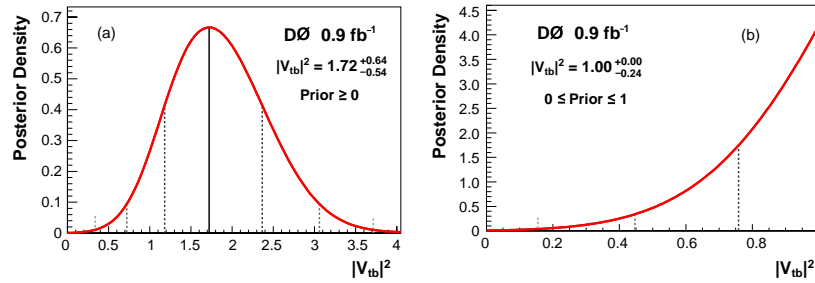

Fig. 3. – The posterior density distributions for $|V_{tb}|^2$ for (a) a nonnegative flat prior, and (b) a flat prior restricted to the region [0,1] and assuming $f_1^L = 1$. The dashed lines show the positions of the one, two, and three standard deviation distances away from the peak of each curve.

We assume that the only production mechanism for single top quarks involves an interaction with a W boson. Therefore, extensions of the SM where single top quark events can be produced, for example, via flavor-changing neutral current interactions or heavy scalar or vector boson exchange, are not considered here. The second assumption is that $|V_{td}|^2 + |V_{ts}|^2 \ll |V_{tb}|^2$. In other words, we assume $|V_{ts}|$ and $|V_{td}|$ are negligible compared to $|V_{tb}|$, without making any assumption on the magnitude of $|V_{tb}|$. Finally, we assume that the Wtb vertex is charge-parity (CP) conserving and of the $V-A$ type, but it is allowed to have an anomalous strength f_1^L. The model independent measurement is

$$|V_{tb}f_1^L| = 1.31^{+0.25}_{-0.21},$$

where f_1^L is a generic left-handed vector coupling. If we constrain the value of $|V_{tb}|$ to the standard model region (i.e., $|V_{tb}| \leq 1$ and $f_1^L = 1$), then at 95% C.L., $|V_{tb}|$ has been measured to be

$$0.68 < |V_{tb}| \leq 1.$$

3. – Search for W' boson resonances decaying to a top quark and a bottom quark

We also report a search for a W' boson that decays to third generation quarks ($W' \to t\bar{b}$ or $\bar{t}b$) [4].

New massive charged gauge bosons, usually called W', are predicted by various extensions of the standard model (SM). Noncommuting extended technicolor, little Higgs, composite gauge bosons, grand unification, and superstring theories represent examples in which an extension of the gauge group leads to the appearance of a W' boson.

A W' boson that decays to tb contributes to single top quark production for which evidence has been reported recently [2]. Since the SM W boson and a hypothetical W' boson with left-handed couplings both couple to the same fermion multiplets, they interfere with each other. The interference term may reduce the total rate by as much as (16–33)%, depending on the mass of the W' boson and its couplings.

The most general lowest-order effective Lagrangian for the interactions of a W' boson with SM fermions f with generation indices i and j, is

$$\mathcal{L} = \frac{V_{ij}}{2\sqrt{2}} g_w \overline{f}_i \gamma^\mu \big[a_{ij}^R (1 + \gamma^5) + a_{ij}^L (1 - \gamma^5) \big] W'_\mu f_j + \text{h.c.},$$

where V_{ij} is the Cabibbo-Kobayashi-Maskawa matrix element if the fermion is a quark, and $V_{ij} = \delta_{ij}$ if it is a lepton, δ_{ij} is the Kronecker delta, g_w is the weak coupling constant of the SM, and a_{ij}^L, a_{ij}^R are coefficients. In this notation, $a_{ij}^L = 1$ and $a_{ij}^R = 0$ for a so-called SM-like W' boson. This effective Lagrangian has been incorporated into the COMPHEP package and used by the SINGLETOP event generator. SINGLETOP is used to simulate SM single top quark production via the exchange of a W boson in the s- and t-channel, and the s-channel W' signal, including interference with the SM W boson. We simulate the complete chain of W', top quark, and W boson decays, taking into account finite widths and all spin correlations between the production of resonance states and their decay. We generate samples of purely left-handed W'_L bosons with $a_{ij}^L = 1$ and $a_{ij}^R = 0$, and purely right-handed W'_R bosons with $a_{ij}^L = 0$ and $a_{ij}^R = 1$. W'_L bosons interfere with the standard W boson, but W'_R bosons couple to different final state particles and therefore do not interfere with the standard W boson. The $\ell\nu$ decays of W'_R bosons involve a right-handed neutrino of unknown mass, assumed to be $M_{\nu_R} > M_{W'}$ or $M_{\nu_R} < M_{W'}$.

The W' width varies between 20 GeV and 30 GeV for W' masses between 600 GeV and 900 GeV. If $M_{\nu_R} > M_{W'}$ and only $q\overline{q'}$ final states are open, the width is about 25% smaller. This does not have a significant effect on our search as the experimental resolution for the tb invariant mass is much larger (≈ 90 GeV). The branching fraction for $W' \to tb$, is around 0.32 (0.24) for decays only to quarks (quarks and leptons) for a W' boson with a mass of 700 GeV and varies slightly with the mass. In the absence of interference between W and W' bosons, and if $M_{\nu_R} < M_{W'}$, there is no difference between W'_L and W'_R for our search. Since the current lower limit on the mass of the W'

boson is around 600 GeV, we simulate W'_L and W'_R bosons at seven mass values from 600 to 900 GeV to probe for W' bosons with higher masses.

We set upper limits on the W' boson production cross section times branching fraction to the tb final state, $\sigma(p\bar{p} \rightarrow W') \times \mathrm{B}(W' \rightarrow tb)$, using the high tail of the $\sqrt{\hat{s}}$ distribution. The uncertainties for this analysis are same as single top analysis [2].

The observed 95% C.L. upper limit of $\sigma(p\bar{p} \rightarrow W') \times \mathrm{B}(W' \rightarrow tb)$ compared to the NLO theory predictions are shown in Fig. 4 for (a) W'_L and (b) W'_R production cross sections. Limits for the gauge couplings $g' = g_w a_{ij}^L$ or $g' = g_w a_{ij}^R$, depending on the model, of the W' boson can be derived from the cross section limits. Since the leading-order s-channel production diagram has two $W'q\bar{q}'$ vertices, $\sigma(p\bar{p} \rightarrow W') \times \mathrm{B}(W' \rightarrow tb)$ is proportional to g'^4. Figure 4(c) shows the observed limit for g'/g_w. We exclude gauge couplings above 0.68 (0.72) g_w for W' bosons with a mass of 600 GeV for the case $M_{\nu_R} > M_{W'}$ ($M_{\nu_R} < M_{W'}$).
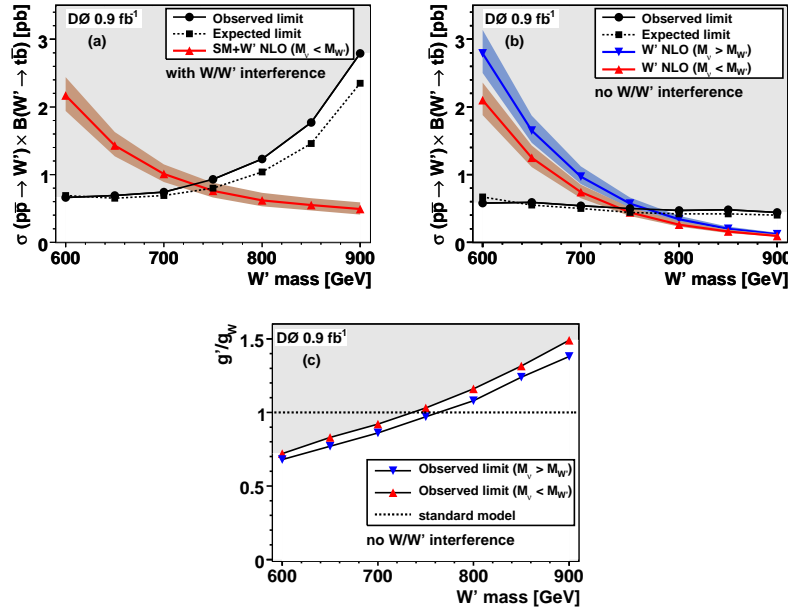

Fig. 4. – NLO theory cross sections and 95% C.L. limits for $\sigma_{W'} \times \mathrm{B}(W' \rightarrow tb)$ as a function of W' mass for (a) W'_L production and (b) W'_R production. Observed limits on the ratio of coupling constants g'/g_w are shown in (c). The shaded regions are excluded by this analysis.

4. – Search for charged Higgs bosons decaying to top and bottom quarks

In the standard model (SM), one $SU(2)$ doublet induces electroweak symmetry breaking, which leads to a single elementary scalar particle: the neutral Higgs boson. Two $SU(2)$ doublets perform the task of electroweak symmetry breaking in two-Higgs-doublet models (2HDMs) [5]. This leads to five physical Higgs bosons among which two carry charge. Hence the discovery of a charged Higgs boson would be unambiguous evidence of new physics beyond the SM. Various types of 2HDMs are distinguished by their strategy

for avoiding flavor-changing neutral currents (FCNCs). In a Type I 2HDM, only one of these doublets couples to fermions. In a Type II 2HDM, a symmetry is imposed so that one doublet couples to up-type fermions and the other couples to down-type fermions; an idea that is augmented in minimal supersymmetry extensions [5]. In a Type III 2HDM, both doublets couple to fermions, no symmetry is imposed, and FCNCs are avoided by other methods.

We present the first search for a charged Higgs boson (H^+) directly produced by quark-antiquark annihilation, and decaying into the $t\bar{b}$ final state, in the $180 \leq M_{H+} \leq 300$ GeV mass range. In most models this decay dominates others for large regions of parameter space when the H^+ mass (M_{H+}) is greater than the mass of the top quark (m_t). Exploring the mass range $M_{H+} > m_t$ is complementary to previous Tevatron searches [6] that have been performed in top quark decays, hence for the $M_{H+} < m_t$ region. This search is also based on the same 0.9 fb^{-1} of data used for single top quark analysis [2].

We use the program CompHEP to simulate charged Higgs boson production and decay $q\bar{q}' \to H^+ \to t\bar{b} \to W b\bar{b}$. This is done for seven M_{H+} values ranging from 180 to 300 GeV. The lower mass value is dictated by the kinematics of the decay $H^+ \to t\bar{b}$ which requires $M_{H+} > m_t + m_b$, where m_b is the mass of the bottom quark. The upper mass value is chosen based on the fact that, in this mass range, the production cross section decreases by approximately an order of magnitude for any of the models considered. During signal event generation, the W boson from the final state top quark decay is forced to decay leptonically. The couplings are set to produce pure chiral state samples that are combined in different proportions to simulate the desired 2HDM type. The interference term proportional to the product of the left and right-handed couplings is smaller than the percent level in the Type I 2HDM, and is considered negligible. The interference term is in the percent level in the $\tan\beta < 30$ region, for the Type II 2HDM, and non-relevant for the Type III 2HDM. Each choice of couplings determines the total width, Γ_{H+}, and the initial-state quark flavor composition. This quark flavor composition of the signal samples is determined by the value of the element $|V_{ij}|$ of the Cabibbo-Kobayashi-Maskawa (CKM) matrix and the CTEQ6L1 parton distribution functions (PDFs). In these simulated signal samples, Γ_{H+} ranges from approximately 4 GeV for $M_{H+} = 180$ GeV to 9 GeV for $M_{H+} = 300$ GeV. We use the same selection as single top analysis except that require exactly two jets. A distinctive feature of signal events is the large mass of the charged Higgs boson. We therefore use the reconstructed invariant mass of the top and bottom quark system as the discriminating variable for the charged Higgs signal.

The systematic uncertainties on the signal and background model are estimated using the methods described in Ref. [2]. For the H^+ signal, the uncertainty on the model-dependent proportion of initial-state parton flavor contribution plays a dominant role. A value of 10% is assigned based on variations in yield and shape of the reconstructed invariant mass distribution.

We observe no excess of data over background and so proceed to set upper limits on H^+ boson production using invariant mass distribution and the same Bayesian approach used above.

The $\sigma \times \mathcal{B}$ upper limits obtained are compared to the expected signal cross section in the Type I 2HDM to exclude a region of the M_{H+} and $\tan\beta$ parameter space, shown in Fig. 5. The analysis sensitivity is currently not sufficient to exclude regions of $\tan\beta < 100$ in the Type II 2HDM.

* * *

Fig. 5. – The 95% C.L. excluded region in the M_{H^+} vs $\tan\beta$ space for Type I 2HDM.

REFERENCES

[1] F. ABE *et al.* (CDF COLLABORATION), *Phys. Rev. Lett.*, **74** (1995) 2626; S. ABACHI *et al.* (D0 COLLABORATION), *Phys. Rev. Lett.*, **74** (1995) 2632.

[2] V.M. ABAZOV *et al.* (D0 COLLABORATION),, *Phys. Rev. Lett.*, **98** (2007) 181802; arXiv.org:0803.0739, submitted to Phys. Rev. D and refrences therein.

[3] Z. SULLIVAN, *Phys. Rev. D*, **70** (2004) 114012.

[4] V.M. ABAZOV *et al.* (D0 COLLABORATION),, *Phys. Rev. Lett.*, **100** (2008) 211803 and refrences therein.

[5] J. GUNION *et al.*,, *The Higgs Hunter's Guide, Frontiers in Physics* ADDISON-WESLEY, REDWOOD 1990.

[6] B. ABBOTT *et al.* (D0 COLLABORATION),, *Phys. Rev. Lett.*, **82** (1999) 4975; V.M. ABAZOV *et al.* (D0 COLLABORATION),, *Phys. Rev. Lett.*, **88** (2002) 151803; A. ABULENCIA *et al.* (CDF COLLABORATION),, *Phys. Rev. Lett.*, **96** (2006) 042003.